LIQUEFACTION POTENTIAL INDEX: A CRITICAL ASSESSMENT USING PROBABILITY CONCEPT

David Kun Li [1], C. Hsein Juang [2], Ronald D. Andrus [3]

ABSTRACT

Liquefaction potential index (I_L) was developed by Iwasaki *et al.* in 1978 to predict the potential of liquefaction to cause foundation damage at a site. The index attempted to provide a measure of the severity of liquefaction, and according to its developer, liquefaction risk is very high if $I_L > 15$, and liquefaction risk is low if $I_L \leq 5$. Whereas the simplified procedure originated by Seed and Idriss in 1971 predicts what will happen to a soil element, the I_L predicts the performance of the whole soil column and the consequence of liquefaction at the ground surface. Several applications of the I_L have been reported by engineers in Japan, Taiwan, and the United States, although the index has not been evaluated extensively. In this paper, the I_L is critically assessed for its use in conjunction with a cone penetration test (CPT)-based simplified method for liquefaction evaluation. Emphasis of the paper is placed on the appropriateness of the formulation of the index I_L and the calibration of this index with a database of case histories. To this end, the framework of I_L by Iwasaki *et al.* is maintained but the effect of using different models of a key component in the formulation is explored. The results of the calibration of I_L are presented. Moreover, use of I_L is extended by introducing an empirical formula for assessing the probability of liquefaction-induced ground failure.

Key words: liquefaction, earthquakes, cone penetration test, case histories, liquefaction potential index, factor of safety, probability of liquefaction.

1. INTRODUCTION

The Liquefaction Potential Index, denoted herein as I_L, was developed by Iwasaki *et al.* (1978, 1981, 1982) for predicting the potential of liquefaction to cause foundation damage at a site. In Iwasaki *et al.* (1982), the index I_L was interpreted as follows: Liquefaction risk is very low if $I_L = 0$; low if $0 < I_L \leq 5$; high if $5 < I_L \leq 15$; and very high if $I_L > 15$. However, the meaning of the word "risk" in the above classification was not clearly defined. Because the index was intended for measuring the liquefaction severity, other interpretations were proposed. For example, Luna and Frost (1998) offered the following interpretation: Liquefaction severity is little to none if $I_L = 0$; minor if $0 < I_L \leq 5$; moderate if $5 < I_L \leq 15$; and major if $I_L > 15$. Moreover, some investigators have tried to correlate the index I_L with surface effects such as lateral spreading, ground cracking, and sand boils (Toprak and Holzer, 2003), and with ground damage near foundations (Juang *et al.,* 2005a). Nevertheless, the interpretation and use of the index I_L can be accepted only if this index is properly calibrated with field data. In this paper, the index I_L is re-assessed and its use is expanded.

Because the focus herein is the severity of liquefaction, the term "liquefaction-induced ground failure," identified by surface manifestations such as sand boils, lateral spreading, and settlement caused by an earthquake, is used through out this paper. Whenever no confusion is created, the term "liquefaction-induced ground failure" is simply referred to herein as "ground failure". Thus, cases from past earthquakes where surface evidence of "liquefaction-induced ground failure" was observed are referred to herein as "ground-failure" cases, and cases without such observed surface manifestations are referred to as "no-failure" cases.

2. LIQUEFACTION POTENTIAL INDEX — AN OVERVIEW

The liquefaction analysis by means of the liquefaction potential index I_L defined by Iwasaki *et al.* (1982) is different from the simplified procedure of Seed and Idriss (1971). The simplified procedure predicts what will happen to a soil element, the index I_L predicts the performance of the whole soil column and the consequence of liquefaction at the ground surface (Lee and Lee, 1994; Lee *et al.,* 2001; Chen and Lin, 2001; Kuo *et al.,* 2001; Toprak and Holzer, 2003). The following assumptions were made by Iwasaki *et al.* (1982) in formulating index I_L:

(1) The severity of liquefaction is proportional to the thickness of the liquefied layer,
(2) The severity of liquefaction is proportional to the proximity of the liquefied layer to the ground surface, and
(3) The severity of liquefaction is related to the factor of safety (FS) against the initiation of liquefaction but only the soils with FS < 1 contribute to the severity of liquefaction.

Conceptually, these assumptions are all considered valid. Furthermore, the effect of liquefaction at depths greater than 20 m is assumed to be negligible, since no surface effects from liquefaction at such depths have been reported. Iwasaki *et al.* (1982) proposed the following form for the index I_L that reflects the stated assumptions:

$$I_L = \int_0^{20} F\, w(z)\, dz \tag{1}$$

Manuscript received May 18, 2005; revised October 7, 2005; accepted October 21, 2005.

[1] Staff Geotechnical Engineer, Golder Associates, Inc., 24 Commerce St., Suite 430, Newark, NJ 07102, U.S.A. (Formerly, Research Assistant, Dept. of Civil Engineering, Clemson University)
[2] Professor (corresponding author), Department of Civil Engineering, Clemson University, Clemson, SC 29634-0911, U.S.A. (e-mail: hsein@clemson.edu).
[3] Associate Professor, Department of Civil Engineering, Clemson University, Clemson, SC 29634-0911, U.S.A.

where the depth weighting factor, $w(z) = 10 - 0.5z$ where z = depth (m). The weighting factor is 10 at $z = 0$, and linearly decreased to 0 at $z = 20$ m. The form of this weighting factor is considered appropriate for the following reasons: (1) the linear trend is considered appropriate since there is no evidence to support the use of high-order functions, (2) the linearly decreasing trend is a reasonable implementation of the second assumption, and (3) the calculated I_L values eventually have to be calibrated with field observations. The variable F is a key component in Eq. (1), and at a given depth, it is defined as follows: $F = 1 - \text{FS}$, for $\text{FS} \le 1$; and $F = 0$ for $\text{FS} > 1$. This definition is of course a direct implementation of the third assumption. Whereas these assumptions were considered appropriate and the calculated I_L values were eventually calibrated with field observations, the general applicability of this approach may be called into question because different FS values may be obtained for the same case using different deterministic models of FS.

In the formulation presented in Iwasaki *et al.* (1982), the factor of safety (FS) was determined using a standard penetration test (SPT)-based simplified method established by the Japan Road Association (1980). The uncertainty of this model by the Japan Road Association, referred to herein as the JRA model, is unknown; in other words, the "true" meaning of the calculated FS is unknown. Even without any parameter uncertainty, there is no certainty that a soil with a calculated FS = 1 will liquefy because the JRA model is most likely a "conservative" model. As with typical geotechnical practice, the deterministic model is almost always formulated so that it is biased toward the conservative side, and thus, FS = 1 generally does not coincide with the limiting state where liquefaction is just initiated. For example, the SPT-based simplified model by Seed *et al.* (1985) was characterized with a mean probability of about 30% (Juang *et al.*, 2002), which means that a soil with FS = 1 has a 30% probability, rather than the "unbiased" 50% probability, of being liquefied. Since the model uncertainty of the JRA model is unknown, the applicability of the criteria established by Iwasaki *et al.* (1982) is quite limited.

In this paper, the definition of I_L is revisited and re-calibrated with a focus on the variable F. Here, F may be derived from the factor of safety, as in the original formulation by Iwasaki *et al.* (1982), or derived from the probability of liquefaction, a new concept developed in this study. In the former approach, four deterministic models of FS, each with a different degree of conservativeness, are used to define the variable F and then incorporated into Eq. (1) for I_L. In the latter approach, only one formulation of F is used, since it is defined with the probability of liquefaction and thus, the issues of model uncertainty and degree of conservativeness are muted. The effectiveness of the two definitions of the variable F, in terms of the ability of the resulting I_L to distinguish "ground-failure" cases from "no-failure" cases, is investigated.

3. DETERMINISTIC MODELS FOR FACTOR OF SAFETY

The factor of safety against the initiation of liquefaction of a soil under a given seismic loading is generally defined as the ratio of cyclic resistance ratio (CRR), which is a measure of liquefaction resistance, over cyclic stress ratio (CSR), which is a representation of seismic loading that causes liquefaction. Symbolically, FS = CRR/CSR. The reader is referred to Seed and Idriss (1971), Youd *et al.* (2001), and Idriss and Boulanger (2004) for historical perspective of this approach. The term CSR is calculated in this paper as follows (Idriss and Boulanger, 2004):

$$\text{CSR} = 0.65\left(\frac{\sigma_v}{\sigma_v'}\right)\left(\frac{a_{\max}}{g}\right)(r_d) / \text{MSF} / K_\sigma \tag{2}$$

where σ_v is the vertical total stress of the soil at the depth considered (kPa), σ_v' the vertical effective stress (kPa), $a_{\max}$ the peak horizontal ground surface acceleration (g), g is the acceleration of gravity, r_d is the depth-dependent shear stress reduction factor (dimensionless), MSF is the magnitude scaling factor (dimensionless), and K_σ is the overburden correction factor (dimensionless).

In Eq. (2), CSR has been adjusted to the conditions of M_w (moment magnitude) = 7.5 and σ_v' = 100 kPa. Such adjustment makes it easier to process case histories from different earthquakes and with soils of concern at different overburden pressures (Juang *et al.,* 2003). It should be noted that in this paper, the terms r_d, MSF, and K_σ are calculated with the formulae recommended by Idriss and Boulanger (2004), as shown in Appendix *I*. A sensitivity analysis, not shown here, reveals that CSR determined with this set of formulae, by Idriss and Boulanger (2004), agrees quite well with that obtained using the "lower-bound" formulae recommended by Youd *et al.* (2001).

The term CRR is calculated using cone penetration test (CPT) data. The following empirical equation developed by Juang *et al.* (2005b) is used here:

$$\text{CRR} = \exp[-2.88 + 0.000309(q_{c1N,m})^{1.8}] \tag{3}$$

where $q_{c1N,m}$ is the stress-normalized cone tip resistance q_{c1N} adjusted for the effect of "fines" on liquefaction (thus, $q_{c1N,m} = K\, q_{c1N}$). The stress-normalized cone tip resistance q_{c1N} used herein follows the definition by Idriss and Boulanger (2004), although the difference between this definition and that by Robertson and Wride (1998) is generally small. The adjustment factor K is computed as:

$$K = 1 \qquad \text{for } I_c < 1.64 \tag{4a}$$

$$= 1 + 80.06(I_c - 1.64)(q_{c1N})^{-1.2194} \qquad \text{for } 1.64 \le I_c \le 2.38 \tag{4b}$$

$$= 1 + 59.24(q_{c1N})^{-1.2194} \qquad \text{for } I_c > 2.38 \tag{4c}$$

Both I_c and q_{c1N} in Eq. (4) are dimensionless. The term I_c is the soil behavior type index (see Appendix I for formulation used in this paper). Although I_c was initially developed for soil classification, use of I_c to "gauge" the effect of "fines" on liquefaction resistance is well accepted (Robertson and Wride, 1998; Youd *et al.,* 2001; Zhang *et al.,* 2002; Juang *et al.,* 2003). In Eq. (4), I_c has lower and upper bounds. If $I_c < 1.64$ (lower bound), it is set to be equal to 1.64, and thus, $K = 1$ (Eq. (4b) becomes (4a)). On the other hand, if $I_c > 2.38$ (upper bound), it is set to be equal to 2.38, and Eq. (4b) becomes Eq. (4c) where K is a function of only q_{c1N}. Equation (4) was established from the adopted database with q_{c1N} values ranging from about 10 to 200, and thus, it is convenient and conservative to set a lower bound of $q_{c1N} = 15$ for

the determination of K. With the aforementioned conditions, the K value ranges from 1 to about 3.

Moreover, according to published empirical equations (Lunne *et al.,* 1997; Baez *et al.,* 2000), I_c = 1.64 corresponds approximately to a fines content (FC) of 5%, and I_c = 2.38 corresponds approximately to FC = 35%. Thus, the three "classes" of liquefaction boundary curves (CRR model) implied by Eqs. (3) and 4 (based on the lower and upper bounds of I_c) are consistent with the commonly defined "classes" of boundary curves, namely, FC < 5%, 5% ≤ FC ≤ 35%, and FC > 35% (Seed *et al.,* 1985; Andrus and Stokoe, 2000).

It is noted that the adjustment factor K proposed in Eq. (4) is a function of not only "fines content" (or more precisely, I_c) but also q_{c1N}. The form of Eq. (4) was inspired by the form of the "equivalent clean soil" adjustment factor successfully adopted for the shear wave velocity-based liquefaction evaluation (Andrus *et al.,* 2004). It should be emphasized, however, that the adjustment factor K defined in Eq. (4) has no physical meaning; it is merely an empirical factor to account for the effect of fines (or I_c) on liquefaction resistance based on case histories.

In summary, the factor of safety against the initiation of liquefaction is calculated as FS = CRR/CSR, where CRR is determined with Eq. (3) and CSR is determined with Eq. (2). The FS calculated for any given depth is then incorporated into Eq. (1) to determine the liquefaction potential index I_L.

4. CALIBRATION OF INDEX I_L DEFINED THROUGH FACTOR OF SAFETY

To calibrate the calculated I_L values, a database of 154 CPT soundings with field observations of liquefaction/no-liquefaction in various seismic events (Table 1) is used. The moment magnitude of these earthquakes ranges from 6.5 to 7.6. Cases with observed liquefaction-induced ground failure (*i.e.*, the occurrence of liquefaction) are referred to as "failure cases," and those without are referred to as "no-failure cases." Among the 154 cases, one half of them (77 cases) are no-failure cases and the other half (77 cases) are failure cases. The CPT sounding logs for these cases are available from the references listed in Table 1 or from the authors upon request.

Figure 1 shows an example calculation of I_L with a CPT sounding. Using Eq. (2), the CSR is calculated, and using Eq. (3) and CPT data, the CRR is calculated, and then FS is calculated and the profile of FS is established. The index I_L is then determined by Eq. (1). It is noted that if the CPT sounding does not reach 20 m, engineering judgment should be exercised to ascertain the potential contribution of the soils below the sounding record to the index I_L. If the contribution is judged to be little to none, the calculated I_L is considered acceptable; otherwise, the case is discarded. Over 200 cases of CPT sounding were "screened" initially in this study, and the 154 cases listed in Table 1 are those that passed screening.

Table 1 Historic field liquefaction effect data with CPT measurements

Site	Sounding ID	Sounding Depth (m)	a_{max} (g)	Observation	Reference
1975 Haicheng earthquake (M_w = 7.3)					
Fisheries and Shipbuilding	FSS	10.0	0.15	Yes	Arulanandan *et al.* (1986)
1971 San Fernando earthquake (M_w = 6.6)					
Balboa Blvd.	BAL-2	11.4	0.45	No	Bennett (1989)
	BAL-4	10.3	0.45	No	
	BAL-8	10.4	0.45	No	
	BAL-10	11	0.45	No	
Wynne Ave.	WYN-1	15.2	0.51	No	
	WYN-2	15.2	0.51	No	
	WYN-5A	16.1	0.51	No	
	WYN-7A	15.7	0.51	No	
	WYN-10	16.1	0.51	No	
	WYN-11	16.2	0.51	No	
	WYN-12	15	0.51	No	
	WYN-14	15.5	0.51	No	
Juvenile Hall	SFVJH-2	15.6	0.5	Yes	
	SFVJH-4	16.7	0.5	Yes	
	SFVJH-10	16.2	0.5	Yes	
1979 Imperial Valley earthquake (M_w = 6.5)					
Radio Tower	R3	16.9	0.22	No	Bennett *et al.* (1981, 1984)
Vail Canal	TV2	9	0.14	No	Bierschwale and Stokoe (1984)
	V1	12.6	0.14	No	
	V2	12.7	0.14	No	
	V3	13	0.14	No	
	V4	12.9	0.14	No	
	V5	16.5	0.14	No	
McKim Ranch	M1	14.9	0.51	Yes	
	M3	12.9	0.51	Yes	
	M7	11	0.51	Yes	
River Park	RiverPark-2	7.20	0.22	Yes	
	RiverPark-5	5.80	0.22	Yes	
	RiverPark-6	6.00	0.22	Yes	

Table 1 Historic field liquefaction effect data with CPT measurements (continued)

Site	Sounding ID	Sounding Depth (m)	a_{max} (g)	Observation	Reference
1987 Superstition Hills earthquake (M_w = 6.6)					
Heber Road	HeberRoad-1	9.4	0.1	No	Bennett *et al.* (1981)
	HeberRoad-2	13	0.1	No	Holzer *et al.* (1989)
	HeberRoad-3	9	0.1	No	
	HeberRoad-4	14.2	0.1	No	
	HeberRoad-5	6.4	0.1	No	
	HeberRoad-6	14.2	0.1	No	
	HeberRoad-7	10.2	0.1	No	
	HeberRoad-8	10.2	0.1	No	
	HeberRoad-9	7.2	0.1	No	
	HeberRoad-10	7.2	0.1	No	
	HeberRoad-11	8.4	0.1	No	
	HeberRoad-12	8.4	0.1	No	
	HeberRoad-13	7	0.1	No	
	HeberRoad-14	6.6	0.1	No	
	HeberRoad-15	7	0.1	No	
	HeberRoad-16	10	0.1	No	
McKim Ranch	M1	14.9	0.20	No	
	M3	12.9	0.20	No	
	M7	11	0.20	No	
Radio Tower	R1	14.9	0.15	No	
	R3	16.9	0.15	No	
	R4	15.1	0.15	No	
River Park	RiverPark-1	8.00	0.15	No	
	RiverPark-2	7.20	0.15	No	
	RiverPark-3	7.20	0.15	No	
	RiverPark-4	8.00	0.15	No	
	RiverPark-5	5.80	0.15	No	
	RiverPark-6	6.00	0.15	No	
	RiverPark-7	6.00	0.15	No	
	RiverPark-8	5.80	0.15	No	
	RiverPark-9	6.80	0.15	No	
	RiverPark-10	5.80	0.15	No	
	RiverPark-11	5.80	0.15	No	
	RiverPark-12	5.20	0.15	No	
	RiverPark-13	11.60	0.15	No	
	RiverPark-14	4.80	0.15	No	
	RiverPark-15	11.60	0.15	No	
Vail Canal	TV2	9	0.21	No	
	V5	16.5	0.21	No	
1989 Loma Prieta earthquake (M_w = 6.9)					
Pajaro Dunes	PAJ-82	7.6	0.17	No	Bennett and Tinsley (1995)
	PAJ-83	9	0.17	No	Tinsley *et al.* (1998)
Tanimura	TAN-105	19.5	0.13	No	Toprak *et al.* (1999)
Model Airport	AIR-17	15.6	0.26	Yes	
	AIR-18	15.8	0.26	Yes	
	AIR-19	15.8	0.26	Yes	
	AIR-20	15.8	0.26	Yes	
Santa Cruze & Montemey	CMF-3	20.2	0.36	Yes	
County	CMF-5	15.1	0.36	Yes	
Clint Miller Farms	CMF-8	15	0.36	Yes	
Farris	FAR-58	17.9	0.36	Yes	
	FAR-61	15	0.36	Yes	
Jefferson Ranch	JRR-32	20.2	0.21	Yes	
	JRR-33	20.3	0.21	Yes	
	JRR-34	19.3	0.21	No	
	JRR-141	19.5	0.21	Yes	
	JRR-142	19.3	0.21	Yes	
	JRR-144	19.3	0.21	Yes	
Kett	KET-74	11.1	0.47	Yes	
Leonardini	LEN-37	20.1	0.22	Yes	
	LEN-38	20.2	0.22	Yes	
	LEN-39	20.3	0.22	Yes	
	LEN-51	19.3	0.22	Yes	
	LEN-53	19.3	0.22	Yes	
Granite Construction Co.	GRA-124	18.8	0.34	Yes	

Table 1 Historic field liquefaction effect data with CPT measurements (continued)

Site	Sounding ID	Sounding Depth (m)	a_{max} (g)	Observation	Reference
	MCG-128	15	0.26	No	
	MCG-136	16.5	0.26	Yes	
Moss Landing	ML-118	14.00	0.28	Yes	
Scattini	SCA-28	20.30	0.23	Yes	
Silliman	SIL-71	19	0.38	Yes	
1994 Northridge earthquake (M_w = 6.7)					
Balboa Blvd.	BAL-2	11.4	0.84	No	Bennett *et al.* (1998)
Wynne Ave.	WYN-1	15.2	0.51	Yes	Holzer *et al.* (1999)
	WYN-5A	16.1	0.51	Yes	
	WYN-7A	15.7	0.51	Yes	
	WYN-8	15.2	0.51	Yes	
	WYN-11	16.2	0.51	Yes	
	WYN-12	15	0.51	No	
	WYN-14	15.5	0.51	Yes	
1999 Kocaeli earthquake (M_w = 7.4)					
Line 1	L1-03	10.3	0.41	No	Bray and Stewart (2000)
	L1-04	10.2	0.41	No	Bray *et al.* (2002)
	L1-05	10.4	0.41	No	http://peer.berkeley.edu
Site A	CPTA6	9.6	0.41	Yes	
Site C	CPTC1	7	0.41	Yes	
	CPTC3	12.2	0.41	Yes	
	CPTC5	12.7	0.41	Yes	
	CPTC6	11.8	0.41	Yes	
Site G	CPTG1	20	0.41	Yes	
	CPTG2	10.3	0.41	Yes	
Site H	CPTH1	10.1	0.41	Yes	
	CPTH2	20	0.41	Yes	
Site J	CPTJ1	20	0.41	Yes	
	CPTJ2	20	0.41	Yes	
1999 Chi-Chi earthquake (M_w = 7.6)					
Dounan	DN1	20	0.18	Yes	Lee *et al.* (2000)
	DN2	20	0.18	Yes	Lee and Ku (2001)
Zhangbin	BL-C1	20	0.12	Yes	
	BL-C2	20	0.12	Yes	
	BL-C3	20	0.12	No	
	BL-C5	20	0.12	No	
	BL-C6	20	0.12	No	
	LK-0	20	0.12	Yes	
	LK-1	20	0.12	Yes	
	LK-E3	20	0.12	Yes	
	LK-E4	20	0.12	Yes	
	LK-N3	20	0.12	Yes	
	LW-A1	20	0.12	Yes	
	LW-A2	20	0.12	Yes	
	LW-A3	20	0.12	No	
	LW-A5	20	0.12	No	
	LW-A6	20	0.12	Yes	
	LW-A9	20	0.12	No	
	LW-C1	20	0.12	Yes	
	LW-C2	20	0.12	No	
	LW-D2	20	0.12	No	
Nantou	NT-C15	17.5	0.39	Yes	MAA (2000b)
	NT-C16	20	0.39	No	Lin *et al.* (2000)
	NT-C7	20	0.39	Yes	
	NT-C8	17.7	0.39	Yes	
	NT-Y13	15.1	0.39	Yes	Lee *et al.* (2000)
	NT-Y15	16.4	0.39	Yes	Yu *et al.* (2000)
Yuanlin	YL-C19	20	0.18	Yes	MAA (2000a)
	YL-C22	20	0.18	Yes	
	YL-C24	20	0.18	Yes	
	YL-C31	20	0.18	Yes	
	YL-C32	20	0.18	Yes	
	YL-C43	20	0.18	Yes	
	YL-K2	20	0.18	Yes	

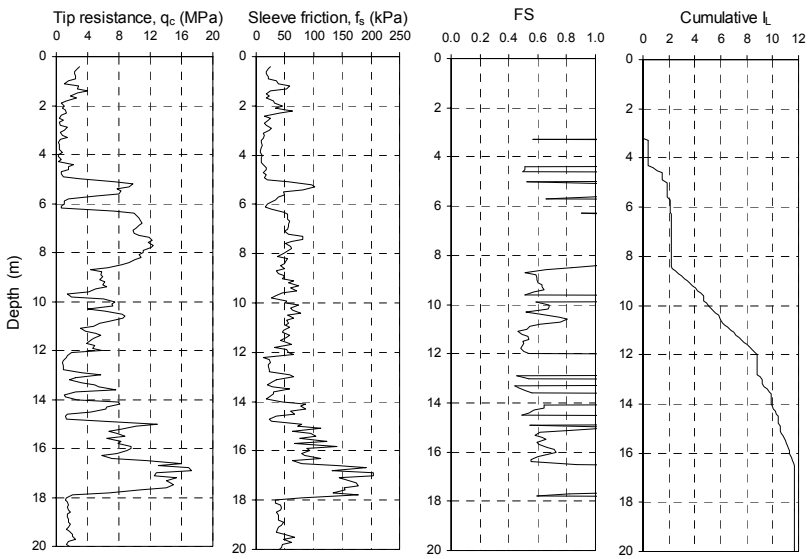

(Sounding ID #DN1; CSR based on the 1999 Chi-Chi earthquake; I_L based on original definition of F)

Fig. 1 CPT sounding profiles and calculation of I_L

Figure 2 shows the distribution of I_L for all 154 cases analyzed. Both histograms and cumulative frequencies of I_L values for the group of ground failure cases, referred to herein as the "failure" group, and that of no ground failure cases, referred to herein as the "no-failure" group, are shown. For the no-failure group, the highest frequency occurs at the lowest I_L class, and as I_L increases, the frequency reduces accordingly. For the failure group, the opposite trend is observed; higher frequency occurs at higher I_L class. It should be noted that in the histograms plotted here, cases with $I_L > 12$ are included in the uppermost class, which makes it easier to examine the range where the failure group and the no-failure group overlapped. Whereas there is an overlap of the two groups, in the range of $I_L = 4$ to 10, the "trend" of both "failure" group and "no-failure" group, in terms of I_L values, is quite clear. For conservative purposes, $I_L = 5$ could be used as a lower bound of failure cases below which no liquefaction-induced ground failure is expected. This result is consistent with the criterion of "$I_L \leq 5$" established by Iwasaki *et al.* (1982) for "low" liquefaction risk. It appears from Fig. 2 that the criterion for "very high" liquefaction risk may be set as "$I_L > 13$", which is quite consistent with the criterion of "$I_L > 15$" established by Iwasaki *et al.* (1982).

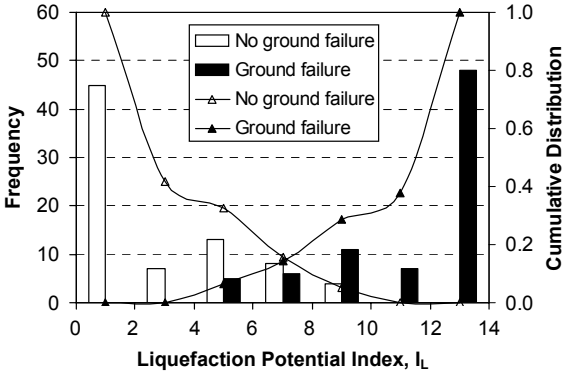

Fig. 2 The distribution of I_L values in both failure and no-failure groups (CRR calculated by Model #3)

The calibration results suggest that the degree of conservativeness of the deterministic model for FS, consisting mainly of Eq. (2) for CSR and Eq. (3) for CRR, happens to be quite consistent with those equations used by Iwasaki *et al.* (1982). For the convenience of further discussion, this deterministic model for FS, or the CRR model (Eq. (3)) for a reference CSR (Eq. (2)), is referred to herein as Model #3 (for reason that would become obvious later). If a deterministic model for FS is more conservative (or less conservative) than Model #3, can the results still be consistent with those criteria established by Iwasaki *et al.* (1982)? Can any deterministic model for FS be incorporated directly into the I_L formulation as defined in Eq. (1) without re-calibration? Previous study by Lee *et al.* (2004) suggested that the I_L index calculated with any new deterministic model for FS needed to be re-calibrated. Obviously, this would hinder the use of the I_L approach for assessing liquefaction severity. In the present study, a series of sensitivity is conducted to investigate this issue.

As noted previously, the deterministic model for liquefaction evaluation is almost always formulated so that it is biased toward the conservative side, and thus, in general, FS = 1 does not correspond to the "true" limit state. For a reference CSR model expressed as Eq. (2), the CRR model expressed as Eq. (3) represents a liquefaction boundary curve. According to Juang *et al.* (2005b), this boundary curve (the CRR model) is characterized with a probability of 24%. In other words, a case with FS = 1 calculated from this deterministic model (Eqs. (2) and (3)) is expected to have a mean probability of liquefaction of 24%. To investigate the effect of the degree of conservativeness of the deterministic model on the calculated I_L index, three additional CRR models are examined. Thus, for the same reference CSR model, the following CRR models are examined in this paper:

$$\text{Model \#1:} \quad \text{CRR} = \exp\left[-2.66 + 0.000309\,(q_{c1N,m})^{1.8}\right] \quad (5a)$$

$$\text{Model \#2:} \quad \text{CRR} = \exp\left[-2.82 + 0.000309\,(q_{c1N,m})^{1.8}\right] \quad (5b)$$

$$\text{Model \#3:} \quad \text{CRR} = \exp\left[-2.88 + 0.000309\,(q_{c1N,m})^{1.8}\right] \quad (5c)$$

$$\text{Model \#4:} \quad \text{CRR} = \exp\left[-2.94 + 0.000309\,(q_{c1N,m})^{1.8}\right] \quad (5d)$$

Equation (5c) is the same as Eq. (3), referred to previously as Model #3. The four CRR models represent boundary curves of the same "family" but with different degrees of conservativeness, as shown in Fig. 3. Model #1 is the least conservative and Model #4 is the most conservative, from the viewpoint of a deterministic evaluation of liquefaction potential based on the calculated FS. Although the derivations using the procedure described in Juang *et al.* (2002) are not shown herein, the boundary curves represented by Models #1, #2, and #4 are characterized by mean probabilities of 50%, 32%, and 15%, respectively. The 50% probability associated with Model #1 implies that this model is essentially an "unbiased" limit state, in reference to the CSR model expressed as Eq. (2). The other three models are all biased toward the conservative side.

Repeating the same analysis as previously carried out using Model #3, the I_L index for each of the 154 cases is calculated using Models #1, #2, and #4. The resulting distributions of the I_L values for the "failure" group and the "no-failure" group are shown in Figs. 4, 5, and 6, respectively, for the corresponding deterministic model (Models #1, #2, and #4 in sequence). From the results shown in Figs. 2, 4, 5, and 6, the following observations are made. Firstly, as the degree of conservativeness of the deterministic model increases (from Model #1 to #4 in sequence), the calculated I_L values gradually becomes larger. The trend is expected; as the calculated FS at any given depth reduces (because a more conservative model is used), the I_L value as per Eq. (1) will increase. This is the primary reason that the calculated I_L needs to be re-calibrated when a different deterministic model for FS is employed, as the meaning of "FS = 1" is different. Secondly, with the smallest calculated I_L values obtained from the least conservative model (Model #1), the distinction between the "failure" group and "no-failure" group based on the calculated I_L values is difficult to establish (see Fig. 4). As the degree of conservativeness of the deterministic model increases, as with Models #2 and #3, the distinction between the two groups becomes easier to make. However, when the most conservative model (Model #4) is employed, the distinction between the two groups is again harder to make. It appears that a deterministic model (boundary curve) that is characterized with a mean probability of approximately 25% to 35% has a better chance to work well with Eq. (1) within the framework developed by Iwasaki *et al.* (1982).

To further interpret the results presented in Fig. 2, which was developed using Model #3 as its deterministic model for FS, Bayes' theorem is employed to estimate the probability of "liquefaction-induced ground failure" based on the distributions of the calculated I_L values of the groups of "failure cases" and "no-failure cases." This approach was suggested by Juang *et al.* (1999) and the probability is calculated as:

$$P_G = P_r(G \mid I_L) \approx \frac{f_F(I_L)}{f_F(I_L) + f_{NF}(I_L)} \tag{6}$$

where the probability of liquefaction-induced ground failure P_G is interpreted as a conditional probability, $P_r(G \mid I_L)$, given a calculated I_L. The approximation in Eq. (6) stems from the assumption that the prior probabilities for ground failure and no-failure, before the determination of I_L, are equal to each other. This assumption is justified, as it is the most likely scenario given the only prior information that there are equal numbers of ground-failure cases and no-failure cases. Thus, the probability of liquefaction-induced ground failure P_G becomes a function of only $f_F(I_L)$ and $f_{NF}(I_L)$, the probability density functions of the calculated I_L of the failure group and the no-failure group, respectively.

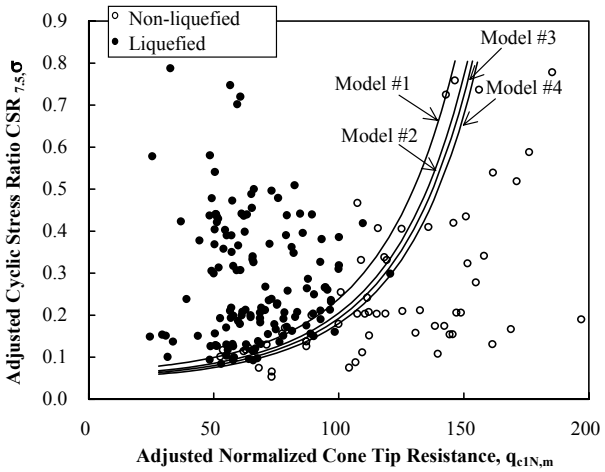

Fig. 3 CRR models with different degrees of conservativeness (Source data: Moss, 2003)

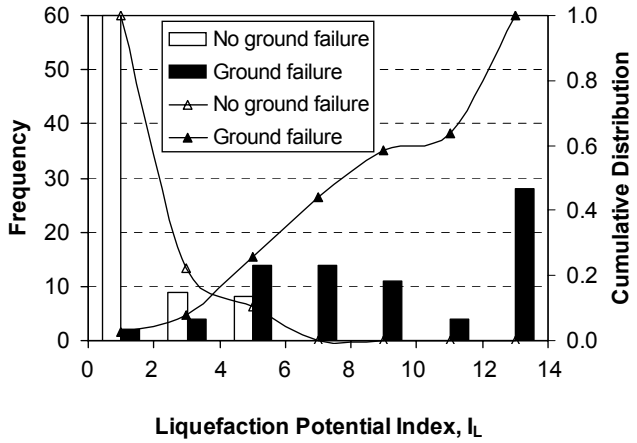

Fig. 4 The distribution of I_L values in both failure and no-failure groups (CRR calculated by Model #1)

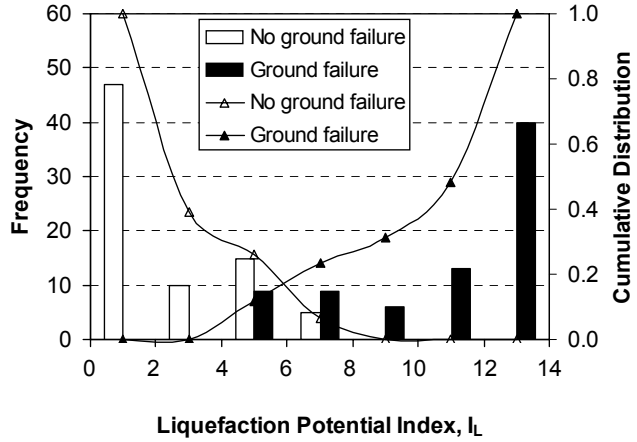

Fig. 5 The distribution of I_L values in both failure and no-failure groups (CRR calculated by Model #2)

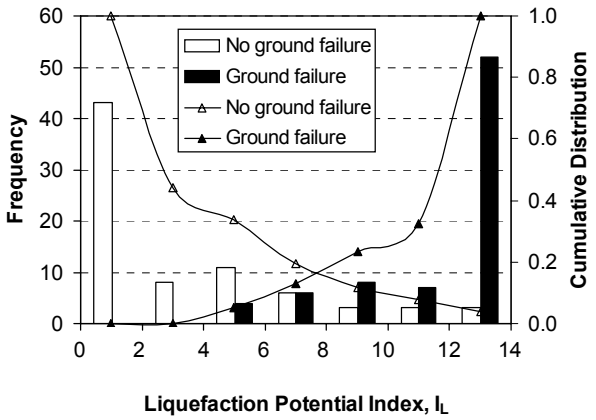

Fig. 6 The distribution of I_L values in both failure and no-failure groups (CRR calculated by Model #4)

Based on the histograms shown in Fig. 2 and the Bayes' theorem as presented in Eq. (6), the relationship between the probability of ground failure P_G and the calculated I_L can be established:

$$P_G = \frac{1}{(1+e^{4.90-0.73I_L})} \tag{7}$$

Figure 7 shows a plot of Eq. (7) along with the data points (P_G, I_L) that were obtained using the procedure (Eq. (6)) described previously. It should be noted that there exist many discrete data points with P_G = 1 or 0; this is easily understood as the overlap of the "failure" group and "no failure" group only falls in the range of I_L = 4 to 10. Thus, all cases with I_L > 10 would have P_G = 1 according to Eq. (6), and all cases with I_L < 4 would have P_G = 0. Although a high coefficient of determination (R^2) is obtained in the curve-fitting, some discrete data points are significantly off the regression curve, as reflected by a significant standard error (ε = 0.073). With Eq. (7), the probability of ground failure P_G can be interpreted for a given I_L calculated from Eq. (1) based on the deterministic model of FS that involves Eqs. (2) and (3).

The significance of the relationship between the probability of ground failure P_G and the calculated I_L, referred herein as the P_G-I_L mapping function, is briefly discussed here. If the index I_L is used directly for assessing liquefaction risk, a different set of criteria has to be pre-calibrated for a different deterministic model of FS that is incorporated into Eq. (1), as is evidenced from the results presented previously. This confirms the previous findings presented by Lee *et al.* (2004). Unlike I_L, however, the probability of liquefaction-induced ground failure provides a "uniform platform" for assessing liquefaction risk. Figure 8 shows the P_G-I_L mapping function obtained from the histograms shown in Fig. 2 (based on Model #3) along with additional P_G-I_L mapping functions obtained from the histograms shown in Fig. 4 (based on Model #1), Fig. 5 (based on Model #2), and Fig. 6 (based on Model #4). With the availability of the P_G-I_L mapping function, only one set of criteria is needed for interpreting the liquefaction risk, regardless of which CRR model is used in the analysis. An example set of criteria is listed in Table 2. With this set of criteria, which is based on the probability of ground failure, a uniform platform for assessing liquefaction risk can be established.

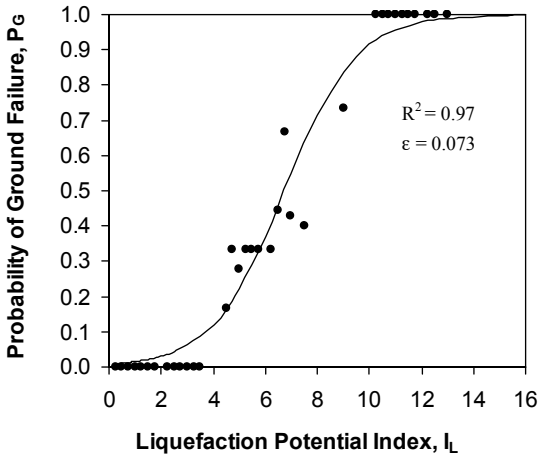

Fig. 7 P_G-I_L relationship (variable F based on factor of safety and CRR by Model #3)

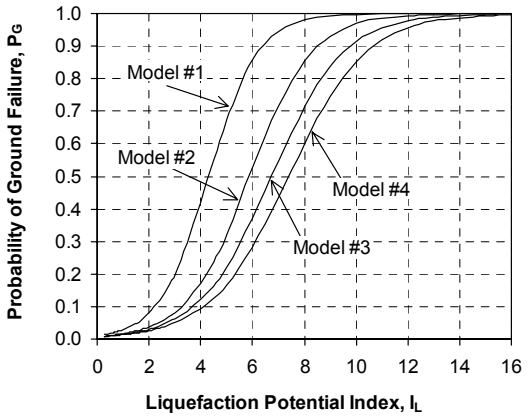

Fig. 8 The P_G-I_L mapping functions (CRR by different models)

Table 2 Probability of liquefaction-induced ground failure

Probability	Description of the risk of liquefaction-induced ground failure
$0.9 < P_G$	extremely high to absolutely certain
$0.7 < P_G \leq 0.9$	high
$0.3 < P_G \leq 0.7$	medium
$0.1 < P_G \leq 0.3$	low
$P_G \leq 0.1$	extremely low to none

Figure 9 shows the P_G values calculated for all 154 cases and the boundary lines that collectively represent this uniform platform for assessing liquefaction risk. Overall, the criteria listed in Table 2 appear to be able to classify both failure cases and no-failure cases. In the class of "extremely high" risk (P_G > 0.9), the percentage of failure cases among all cases in this class, as shown in Fig. 9, is 100%. In the class of "extremely low to none" risk ($P_G \leq 0.1$), the percentage of failure cases among all cases in this class, as shown in Fig. 9, is 0. The overlapping of failure and no-failure cases occurs in the middle three classes. In the class of "high risk" (P_G = 0.7 ~ 0.9), the percentage of failure cases is 71% (10/14) based on the limited data shown in Fig. 9. In the class of "medium risk" (P_G = 0.3 ~ 0.7), the percentage of failure cases is 42% (8/19), and in the class of "low risk" (P_G = 0.1 ~ 0.3), the percentage of failure cases is 23% (3/13). These failure percentages appear to be reasonable for the corresponding classes of risk.

It should be of interest to examine no-failure cases that have a computed P_G value in the range of 0.7 to 0.9 (falling into the class of "high" liquefaction risk) and failures cases that have a computed P_G value in the range of 0.1 to 0.3 (falling in the class of "low" liquefaction risk). Four "no-failure" cases (LW-A3, BL-C3, BL-C5, and BL-C6), shown in the upper right corner of Fig. 9, are found to have $0.7 < I_L < 0.9$. The "predictions" of these cases by means of the calculated P_G values are not accurate, although they represented only 29% of all cases in this range and erred on the safe side. A further examination of these cases revealed that the contributing layers (toward I_L) in these cases were all underneath thick non-contributing layers. The analysis using the procedure recommended by Ishihara (1985), not shown here, actually "predicted" no ground failure in these cases. In other words, in these four cases, lack of surface manifestation observed in the earthquake can be explained with the Ishihara procedure. However, this observation should not be generalized. Overall, the accuracy of the prediction of liquefaction risk using the calculated P_G, as shown in Fig. 9, is quite satisfactory. Nevertheless, the results point to the advantages of using more than one method for evaluating liquefaction risk.

The three failure cases having $0.1 < P_G \leq 0.3$, shown in the lower right corner of Fig. 9, are WYN-1, WYN-11, and SFVJH-10. The first two cases are from the Wynne Avenue site, in San Fernando Valley, California, and the third case is from the Juvenile Hall site, also in San Fernando Valley, California. The geologic setting of the two sites is similar, and thus, the discussion of the first two cases should be applicable to the third case. According to Toprak and Holzer (2003), sites in San Fernando Valley are underlain predominantly by alluvial fan deposits with thin liquefiable silty sand layers and relatively deep groundwater table levels. Thus, the calculated I_L values tend to be low and so is the P_G value. This explains why the assessment based on the calculated P_G value did not agree with field observations. It should be noted that for these cases, the Ishihara procedure did not predict the surface deformation either. In a recent study by Dawson and Baise (2005), the two cases from the Wynne Avenue site were re-assessed based on a three-dimensional interpolation using geostatistics. They concluded that a thin liquefiable layer that is continuous and extends over a large area could lead to ground deformation. This could help explain the observation of surface manifestation for these cases even with a low P_G value.

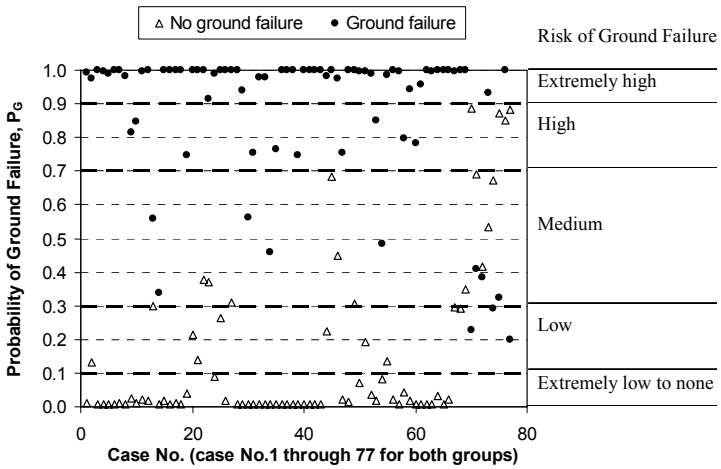

Fig. 9 The distribution of P_G of all 154 cases (CRR by Model #3)

In summary, the accuracy of the assessment based on the calculated P_G is considered satisfactory. The analysis results of a few exceptions indicate, however, the method is not perfect, and use of more than one method for assessing liquefaction risk to increase the accuracy and confidence of the prediction should be encouraged.

5. FURTHER DEVELOPMENT OF INDEX I_L

The results presented previously have established that whenever a new deterministic model of FS is used in Eq. (1), the calculated I_L needs to be re-calibrated and a different set of criteria similar to the one proposed by Iwasaki *et al.* (1982) needs to be established for assessing liquefaction risk. The problem may be overcome by assessing liquefaction risk in terms of the probability of ground failure for a given I_L. In this section, further development of the index I_L is presented. Here, the same formula as expressed in Eq. (1) is used for I_L but the variable F is defined based on the probability of liquefaction rather than the factor of safety at a given depth.

Using Model #3 as an example, CRR is calculated with Eq. (5c) and CSR is calculated with Eq. (2). Then, FS for the soil at a given depth is calculated (FS = CRR/CSR). Recall that a mapping function that maps the calculated FS to the probability of liquefaction (P_L) of the soil at that given depth can be established using Bayes' theorem as outlined by Juang *et al.* (1999, 2002). The mapping function established for the situation where CRR is calculated with Eq. (5c) (Model #3) takes the following form:

$$P_L = \frac{1}{1+\left(\frac{\mathrm{FS}}{0.81}\right)^{5.45}} \tag{8}$$

Using Eq. (8), the probability of liquefaction of a soil at a given depth can be determined based on a calculated FS.

In principle, the probability of liquefaction is a better measure of liquefaction potential than the factor of safety is, and thus, defining the variable F in terms of P_L, rather than FS, may yield a more reasonable and consistent I_L . However, the experience with the variable F that was defined in terms of FS, as reflected in the results of the sensitivity study using Models #1, #2, #3, and #4, suggests that FS = 1 is not necessarily the best choice as a "limiting condition." Thus, in this study, the following definition for the variable F is adopted:

$$F = P_L - 0.35 \qquad \text{if } P_L \geq 0.35$$

$$F = 0 \qquad \text{if } P_L < 0.35 \tag{9}$$

Selection of the threshold probability of 0.35 in the definition of F is briefly discussed in the following. As established previously, a deterministic model that is characterized with a mean probability of approximately 25% to 35% worked well with Eq. (1) within the framework developed by Iwasaki *et al.* (1982). Thus, an appropriate choice for the threshold probability should approximately fall in this range. Of course, the variable F defined in terms of FS, as in the original formulation by Iwasaki *et al.* (1982), has a different effect on the computed I_L than does the one defined in terms of P_L, as in Eq. (9). Ultimately, whether

the definition of F and the associated threshold probability are appropriate depends on the results of calibration with field cases. To this end, a sensitivity study involving use of five different threshold probabilities, including 0.50, 0.35, 0.30, 0.25, and 0.15 is conducted, and the results, not presented herein, show that use of the threshold probability of 0.35 produce the best results.

The threshold probability of 0.35 is also consistent with the classification of liquefaction potential by Chen and Juang (2000), in which the likelihood of liquefaction is considered "low" if P_L < 0.35, and thus, the contribution of a soil layer with P_L < 0.35 to liquefaction-induced ground failure observed at the ground surface may be negligible. Thus, the definition of F involving a threshold probability of 0.35 is recommended. Figure 10 shows an example calculation of I_L with a CPT sounding, similar to that shown in Fig. 1, except that the variable F is calculated with the definition given in Eq. (9).

With the new definition of F given in Eq. (9), the I_L value for each of the 154 cases is calculated. Figure 11 shows the distributions of the I_L values of the "failure" and "no failure" groups. The results are remarkably similar to those presented in Fig. 2 that used the deterministic model of FS (Model #3). Here, the overlap of the two groups is found in the range of I_L = 4 to 10 and the distinction between the "failure" group and the "no-failure" group based on the index I_L is quite clear. The boundary "I_L = 5" may be used as a lower bound of failure cases below which no liquefaction-induced ground failure is expected. Again, this result is consistent with the criterion of "$I_L \leq 5$" established by Iwasaki *et al.* (1982) for "low" liquefaction risk. The lower bound for the class of "very high" liquefaction risk may be taken at I_L = 13, which is slightly lower than the lower bound of "I_L = 15" established by Iwasaki *et al.* (1982). Overall, the results are quite consistent with those of Iwasaki *et al.* (1982) and those presented previously using the deterministic model of FS (Model #3). Significance of the new definition of the variable F, however, lies in the fact that the issue of the effect of model uncertainty of the adopted deterministic model of FS on the calculated I_L and the issue of the degree of conservativeness are muted because in the new definition, F, is based on the probability of liquefaction.

As was done previously, a mapping function that relates the calculated I_L to the probability of ground failure P_G can be obtained based on the histograms shown in Fig. 11. The resulting mapping function takes the following form (see Fig. 12):

$$P_G = \frac{1}{(1+e^{4.71-0.71I_L})} \tag{10}$$

For each of the 154 cases, the index I_L (defined through the new definition of "F") and the probability of ground failure P_G can be calculated. Figure 13 shows the calculated P_G for all 154 cases. Similar to the results presented in Fig. 9, the results obtained based on this new definition of the variable F are generally satisfactorily. In the class of "extremely high" risk (P_G > 0.9), the percentage of failure cases among all cases in this class is 100%. In the class of "little to none" risk ($P_G \leq 0.1$), the percentage of failure cases among all cases in this class is 0. The overlapping of failure and no-failure cases occurs in the middle three classes. In the class of "high risk" (P_G = 0.7 ~ 0.9), the percentage of failure cases is 71% (10/14). In the class of "medium risk" (P_G = 0.3 ~ 0.7), the percentage of failure cases is 47% (7/15), and in the class of "low risk" (P_G = 0.1 ~ 0.3), the percentage of failure cases is 26% (5/19). Overall, the result as reflected in the failure percentages in various classes is deemed reasonable. The results, again, support the criteria presented in Table 2 for interpreting the calculated P_G. Finally, Fig. 14 shows a comparison of the probabilities of ground failure P_G of the 154 cases calculated with Eq. (10) versus those obtained from Eq. (7), which is another way to compare the results presented in Fig. 9 with those

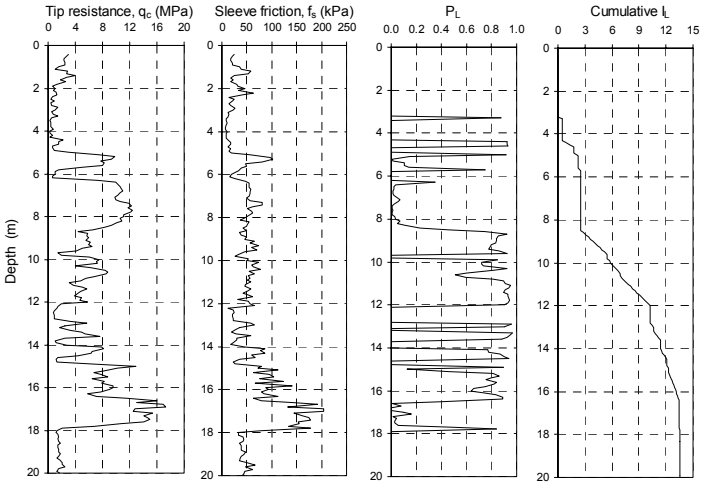

Fig. 10 CPT sounding profiles and calculation of I_L (Sounding ID #DN1; CSR based on the 1999 Chi-Chi earthquake; I_L based on F defined by Eq. (9))

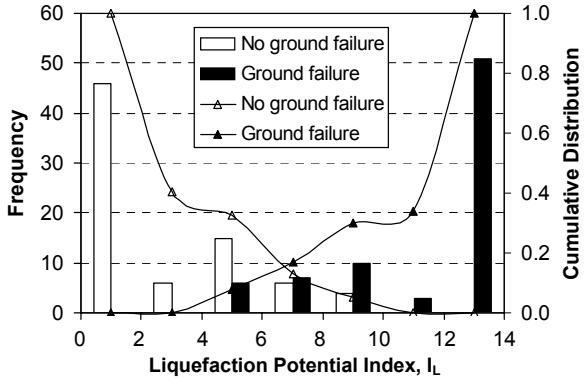

Fig. 11 The distribution of I_L values of the 154 cases (variable F is defined by Eq. (9))

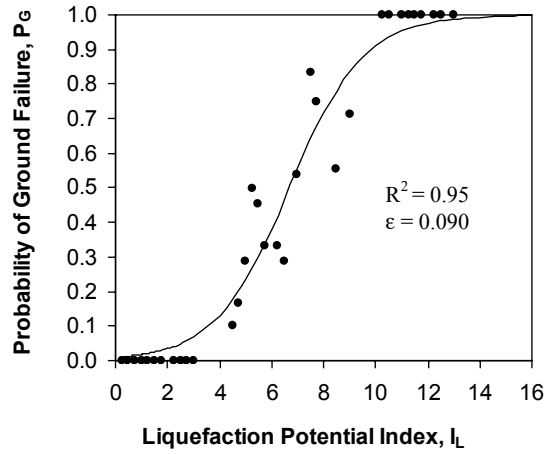

Fig. 12 P_G-I_L relationship (variable F defined by Eq. (9))

shown in Fig. 13. As shown in Fig. 14, the results obtained from both equations agree well with each other, given that the two equations are derived from different concepts (one based on FS and the other based on P_L). Overall, Eq. (10) yields the results that are slightly "better," since it tends to predict higher probabilities for "failure" cases and lower probabilities for "no-failure" cases.

To further demonstrate the developed method (Eq. (10) along with other associated equations), a set of 74 CPTs from the town of Yuanlin, Taiwan compiled by Lee *et al.* (2004) are analyzed for their probabilities of liquefaction-induced ground failure using seismic parameters from the 1999 Chi-Chi earthquake. The reader is referred to Lee *et al.* (2004) for detail of these CPTs and seismic parameters. The contour of the P_G values is prepared and three zones of ground failure potential (high, medium, and low risks) are identified, as shown in Fig. 15. Also shown in this figure are the locations of these CPTs and the sites/areas where liquefaction damage was observed in the town of Yuanlin in the 1999 Chi-Chi earthquake. All but a few spots of the observed liquefaction damage areas are in the "predicted" high risk or medium risk zone. The performance of the developed method is considered satisfactory. Obviously, the accuracy of the ground failure potential map could be improved by increasing the number of well-placed CPT soundings and demanding a more accurate determination of a_{max} at individual locations (instead of using a uniform a_{max} over the entire area). These topics are, however, beyond the scope of this paper.

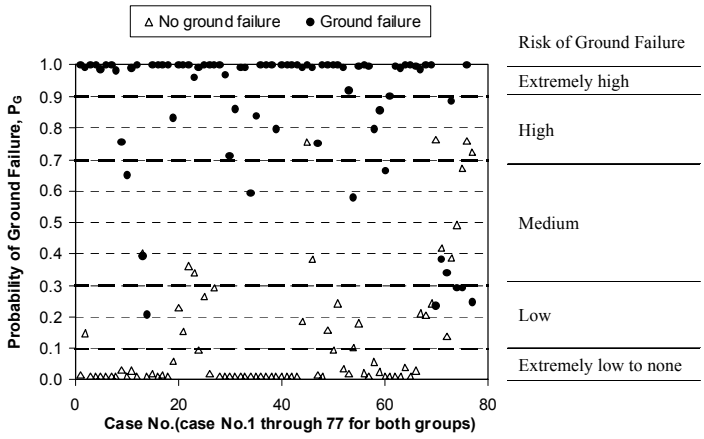

Fig. 13 The distribution of P_G of all 154 cases (variable F by Eq. (9))

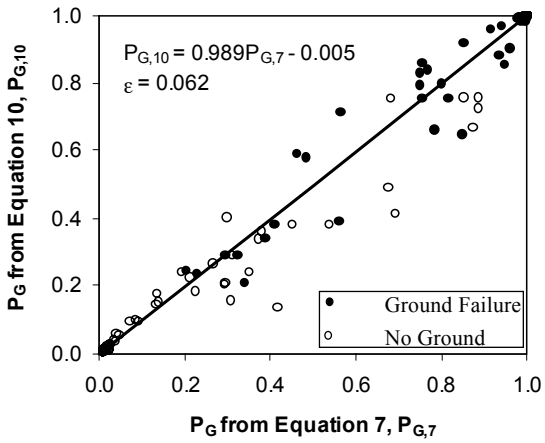

Fig. 14 Comparison of P_G of the 154 cases obtained from different equations

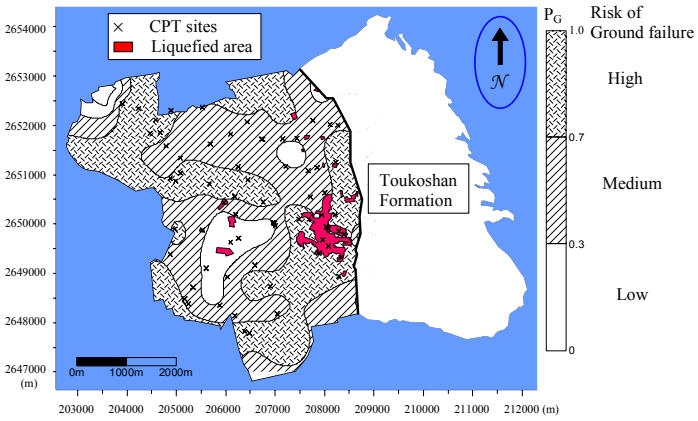

Fig. 15 Liquefaction-induced ground failure potential map for the town of Yuanlin

In summary, the liquefaction potential index developed by Iwasaki *et al.* (1982) has been modified. The modification involves use of a new definition of the variable "F" that is defined based on the probability of liquefaction of a soil at a given depth, instead of the factor of safety. This modification removes the concerns of model uncertainty and degree of conservativeness that are associated with the use of the deterministic model of FS. A mapping function (Eq. (10)) that produces a reasonable estimate of the probability of liquefaction-induced ground failure (P_G) for a given I_L is established. The risk of liquefaction-induced ground failure can be assessed through a set of criteria established based on the calculated P_G (Table 2).

6. CONCLUSIONS

(1) The approach of using the liquefaction potential index (I_L) for assessing liquefaction risk, originated by Iwasaki *et al.* (1982), is shown to be effective through various calibration analyses using 154 field cases. However, the index must be re-calibrated when a different deterministic method is adopted for the calculation of the factor of safety that is the main component of the liquefaction potential index.

(2) Four models of CRR (and thus FS) are examined for their suitability to be incorporated in the framework of I_L. These models are all based on CPT and each with a different degree of conservativeness (*i.e.*, being characterized with a different mean probability, ranging from 15% to 50%). The results of the calibration analyses show that a deterministic FS model that is characterized with a mean probability of approximately 25% to 35% works well with the framework of I_L developed by Iwasaki *et al.* (1982).

(3) A mapping function that links the calculated I_L to the probability of liquefaction-induced ground failure (P_G) is developed. The probability of ground failure provides a "uniform platform" for assessing liquefaction risk. If the I_L is used directly for assessing liquefaction risk, different sets of criteria for interpreting the calculated I_L need to be developed for different models of FS that are incorporated in the framework. Use of the P_G for assessing liquefaction risk requires only one set of criteria such as those given in Table 2.

(4) Further development of the framework of I_L using the probability of liquefaction at a given depth, in lieu of the factor of safety, is conducted in this paper. Use of the probability

of liquefaction to define the variable F in Eq. (1) removes the concerns of model uncertainty and degree of conservativeness that are associated with the use of the deterministic model of FS. Calibration of the calculated I_L and P_G based on this new definition of the variable F yield a result that is as accurate as the best of the previous models in which the variable F was defined in terms of factor of safety. The proposed framework based on the new definition of the variable F is deemed satisfactory as a tool for assessing liquefaction risk.

ACKNOWLEDGMENTS

The study on which this paper is based was supported by the National Science Foundation through Grant CMS-0218365. This financial support is greatly appreciated. The opinions expressed in this paper do not necessarily reflect the view of the National Science Foundation. The database of case histories with CPT soundings that was used in this study was collected from various reports by a number of individuals; their contributions to this paper are acknowledged by means of references cited in Table 1.

REFERENCES

Andrus, R. D. and Stokoe, K. H. (2000). "Liquefaction resistance of soils from shear wave velocity." *J. Geotech. and Geoenvironmental Engrg*., ASCE, 126(11), 1015–1025.

Andrus, R. D., Stokoe, K. H., II, and Juang, C. H. (2004). "Guide for shear-wave-based liquefaction potential evaluation." *Earthquake Spectra*, EERI, 20(2), 285–308.

Arulanandan, K., Yogachandan, C., Meegoda, N. J., Liu, Y., and Sgi, Z. (1986). "Comparison of the SPT, CPT, SV and electrical methods of evaluating earthquake liquefaction susceptibility in Ying Kou City during the Haicheng Earthquake." *Use of In Situ Tests in Geotechnical Engineering*, Geotechnical Special Publication, 6, ASCE, 389–415.

Baez, J. I., Martin, G. R., and Youd, T. L (2000). "Comparison of SPT-CPT liquefaction evaluation and CPT interpretations." *Geotechnical Special Publication*, 97, Mayne, P.W. and Hryciw, R., Eds., ASCE, Reston, Virginia, 17–32.

Bennett, M. J. (1989). "Liquefaction analysis of the 1971 ground failure at the San Fernando Valley Juvenile Hall, California." *Association of Engineering Geology, Bull.*, 26(2), 209–226.

Bennett, M. J., Youd, T. L., Harp, E. L., and Wieczorek, G. F. (1981). *Subsurface Investigation of Liquefaction, Imperial Valley Earthquake, California, October 15, 1979*, U.S. Geological Survey, Open-File Report 81-502, Menlo Park, California.

Bennett, M. J., McLaughlin, P. V., Sarmiento, J. S., and Youd, T. L. (1984). *Geotechnical Investigation of Liquefaction Sites, Imperial Valley, California*, U.S. Geological Survey, Open-File Report 84-252, Menlo Park, California.

Bennett, M. J. and Tinsley, J. C., III (1995). *Geotechnical Data from Surface and Subsurface Samples Outside of and Within Liquefaction-Related Ground Failures Caused by the October 17, 1989, Loma Prieta Earthquake, Santa Cruz and Monterey Counties, California*, U.S. Geological Survey, Open-File Report 95-663, Menlo Park, California.

Bennett, M. J., Ponti, D. J., Tinsley, J. C. III, Holzer, T. L., and Conaway, C. H. (1998). "Subsurface geotechnical investigations near sites of ground deformation caused by the January 17, 1994, Northridge, California, earthquake." U.S. Geological Survey Open-File Rep. 98-373, U.S. Geological Survey, Menlo Park, CA, U.S.A.

Bierschwale, J. G. and Stokoe, K. H., II (1984). "Analytical evaluation of liquefaction potential of sands subjected to the 1981 Westmorland earthquake." Geotechnical Engineering Report GR-84-15, University of Texas at Austin, 231p.

Bray, J. D. and Stewart, J. P. (2000). (Coordinators and Principal Contributors) Baturay, M. B., Durgunoglu, T., Onalp, A., Sancio, R. B., and Ural, D. (Principal Contributors). "Damage patterns and foundation performance in Adapazari." Kocaeli Turkey Earthquake of August 17, 1999 Reconnaissance Report, Chapter 8, Earthquake Spectra, EERI, Supplement A, 16, 163–189.

Bray, J. D., Sancio, R. B., Durgunoglu, H. T., Onalp, A., Stewart, J. P., Youd, T. L., Baturay, M. B., Cetin, K. O., Christensen, C., Emrem, C., and Karadayilar, T. (2002). "Ground failure in Adapazari, Turkey." *Proceedings, Turkey-Taiwan NSF-TUBITAK Grantee Workshop*, Antalya, Turkey.

Chen, C. J. and Juang, C. H. (2000). "Calibration of SPT- and CPT-based liquefaction evaluation methods." *Innovations Applications in Geotechnical Site Characterization*, Mayne, P. and Hryciw, R., Eds., *Geotechnical Special Publication No. 97*, ASCE, New York, 49–64.

Chen, J. C. and Lin, H. H. (2001). "Evaluation of soil liquefaction potential for Kaohsiung metropolitan area." *Proceedings of 9th Conference on Current Research in Geotechnical Engineering*, Taoyuan, Taiwan (in Chinese).

Dawson, K. M. and Baise, L. G. (2005). "Three-dimensional liquefaction potential analysis using geostatistical interpolation." *Soil Dynamics and Earthquake Engineering* (in press).

Holzer, T. L., Youd, T. L., and Hanks, T. C. (1989). "Dynamics of liquefaction during the 1987 Superstition Hills, California, earthquake." *Science*, 244, 56–59.

Holzer, T. L., Bennett, M. J., Ponti, D. J., and Tinsley, J. T., III, (1999). "Liquefaction and soil failure during 1994 Northridge earthquake." *J. Geotechnical and Geoenvironmental Engineering*, 125(6), 438–452.

Idriss, I. M. and Boulanger, R. W. (2004). "Semi-empirical procedures for evaluating liquefaction potential during earthquakes." *Proceedings, Joint Conference, the 11th International Conf. on Soil Dynamics and Earthquake Engineering (SDEE), the 3rd International Conf. on Earthquake Geotechnical Engineering (ICEGE)*, Berkeley, California, 32–56.

Ishihara, K. (1985). "Stability of natural deposits during earthquakes." *Proceedings of the 11th International Conference on Soil Mechanics and Foundation Engineering*, 1, A.A. Balkema, Rotterdam, Netherlands, 321–376.

Iwasaki, T., Tatsuoka, F., Tokida, K., and Yasuda, S. (1978). "A practical method for assessing soil liquefaction potential based on case studies at various sites in Japan." *Proc., 2nd Int. Conf. on Microzonation,* San Francisco, 885–896.

Iwasaki, T., Tokida, K., and Tatsuoka, F. (1981). "Soil liquefaction potential evaluation with use of the simplified procedure." *International Conference on Recent Advances in Geotechnical Earthquake Engineering and Soil Dynamics*, St. Louis, 209–214.

Iwasaki, T., Arakawa, T., and Tokida, K. (1982). "Simplified procedures for assessing soil liquefaction during earthquakes." *Proceedings of the Conference on Soil Dynamics and Earthquake Engineering*, Southampton, UK, 925–939.

Japan, Road Association (1980). "Specifications for Highway

Bridges, Part V. Earthquake Resistant Design." (in Japanese).

Juang, C. H., Rosowsky, D. V., and Tang, W. H. (1999). "Reliability-based method for assessing liquefaction potential of soils." *Journal of Geotechnical and Geoenvironmental Engineering*, ASCE, 125(8), 684−689.

Juang, C. H., Jiang, T., and Andrus, R. D. (2002). "Assessing probability-based methods for liquefaction evaluation." *Journal of Geotechnical and Geoenvironmental Engineering*, ASCE, 128(7), 580−589.

Juang, C. H., Yuan, H., Lee, D. H., and Lin, P. S. (2003). "Simplified CPT-based method for evaluating liquefaction potential of soils." *Journal of Geotechnical and Geoenvironmental Engineering*, ASCE, 129(1), 66−80.

Juang, C. H., Yuan, H., Li, D. K., Yang, S. H., and Christopher, R. A. (2005a). "Estimating severity of liquefaction-induced damage near foundation." *Soil Dynamics and Earthquake Engineering*, (in press).

Juang, C. H., Fang, S. Y., and Li, D. K. (2005b). "Reliability analysis of soil liquefaction potential." *Geotechnical Special Publication,* 133, ASCE, Reston, VA, U.S.A.

Kuo, C. P., Chang, M. H., Chen, J. W., and Hsu, R. Y. (2001). "Evaluation and case studies on liquefaction potential of alluvial deposits at Yunlin county, Taiwan." *Proceedings of 9th Conference on Current Research in Geotechnical Engineering*, Taoyuan, Taiwan (in Chinese).

Lee, H. H. and Lee, J. H. (1994). "A study of liquefaction potential map of Taipei Basin." Technical Report No. GT94003, National Taiwan University of Science and Technology, Taipei, Taiwan.

Lee, D. H., Ku, C. S., and Juang, C. H. (2000). "Preliminary investigation of soil liquefaction in the 1999 Chi-Chi, Taiwan, earthquake." *Proceedings, International Workshop on Annual Commemoration of Chi-Chi Earthquake.* Loh, C.H. and Liao, W.I., Eds., National Center for Research on Earthquake Engineering, Taipei, Taiwan. III, 140−151.

Lee, D. H. and Ku, C. S. (2001). "A study of the soil characteristics at liquefied areas." *Journal of the Chinese Institute of Civil and Hydraulic Engineering*, 13(4), 779−791.

Lee, D. H., Ku, C. S., Chang, S. H., and Wang, C. C. (2001). "Investigation of the post-liquefaction settlements in Chi Chi earthquake." *Proceedings of 9th Conference on Current Research in Geotechnical Engineering*, Taoyuan, Taiwan (in Chinese).

Lee, D. H., Ku, C. S., and Yuan, H. (2004). "A study of the liquefaction risk potential at Yuanlin, Taiwan." *Engineering Geology*, 71(1-2), 97−117.

Lin, P. S., Lai, S. Y., Lin, S. Y., and Hseih, C. C. (2000). "Liquefaction potential assessment on Chi-Chi earthquake in Nantou, Taiwan." *Proceedings, International Workshop on Annual Commemoration of Chi-Chi Earthquake,* Loh, C.H. and Liao, W.I., Eds., National Center for Research on Earthquake Engineering, Taipei, Taiwan, III, 83−94.

Luna, R. and Frost, J. D. (1998). "Spatial liquefaction analysis system." *J. Comput.Civ. Eng.*, 12(1), 48−56.

Lunne, T., Robertson, P. K., and Powell, J. J. M. (1997). *Cone Penetration Testing*. Blackie Academic & Professional, London, UK.

MAA (2000a). *Soil Liquefaction Assessment and Remediation Study, Phase I (Yuanlin, Dachun, and Shetou), Summary Report and Appendixes*. Moh and Associates (MAA), Inc., Taipei, Taiwan (in Chinese).

MAA (2000b). *Soil Liquefaction Investigation in Nantou and Wufeng Areas.* Moh and Associates (MAA), Inc., Taipei, Taiwan (in Chinese).

Moss, R. E. S. (2003). "CPT-based probabilistic assessment of seismic soil liquefaction initiation." Ph.D. Dissertation, University of California, Berkeley, CA, U.S.A.

Robertson, P. K. and Wride, C. E. (1998). "Evaluating cyclic liquefaction potential using the cone penetration test." *Canadian Geotechnical Journal*, 35(3), 442−459.

Seed, H. B. and Idriss, I. M. (1971). "Simplified procedure for evaluating soil liquefaction potential." *Journal of the Soil Mechanics and Foundation Div*., ASCE, 97(9), 1249−1273.

Seed, H. B., Tokimatsu, K., Harder, L. F., and Chung, R. (1985). "Influence of SPT procedures in soil liquefaction resistance evaluations." *Journal of Geotechnical Engineering*, ASCE, 111(12), 1425−1445.

Tinsley, J. C., III, Egan, J. A., Kayen, R. E., Bennett, M. J., Kropp, A., and Holzer, T. L. (1998). "Strong ground and failure, appendix: maps and descriptions of liquefaction and associated effects." *The Loma Prieta, California, Earthquake of October 17, 1989: Liquefaction*, Holzer, T.L., Ed., United States Government Printing Office, Washington, B287−B314.

Toprak, S., Holzer, T. L., Bennett, M. J., and Tinsley, J. C., III (1999). "CPT- and SPT-based probabilistic assessment of liquefaction." *Proceedings of Seventh US-Japan Workshop on Earthquake Resistant Design of Lifeline Facilities and Counter-Measures Against Liquefaction*, Seattle, August 1999, Multidisciplinary Center for Earthquake Engineering Research, Buffalo, NY, U.S.A., 69−86.

Toprak, S. and Holzer, T. L. (2003). "Liquefaction potential index: field assessment." *Journal of Geotechnical and Geoenvironmental Engineering*, ASCE, 129(4), 315−322.

Youd, T. L., Idriss, I. M., Andrus, R. D., Arango, I., Castro, G., Christian, J. T., Dobry, R., Liam Finn, W. D., Harder, L. F., Jr., Hynes, M. E., Ishihara, K., Koester, J. P., Laio, S. S. C., Marcuson, W. F., III, Martin, G. R., Mitchell, J. K., Moriwaki, Y., Power, M. S., Robertson, P. K., Seed, R. B., and Stokoe, K. H., II. (2001). "Liquefaction resistance of soils: summary report from the 1996 NCEER and 1998 NCEER/NSF workshops on evaluation of liquefaction resistance of soils." *Journal of Geotechnical and Geoenvironmental Engineering*, ASCE, 127(10), 817−833.

Yu, M. S., Shieh, B. C., and Chung, Y. T. (2000). "Liquefaction induced by Chi-Chi earthquake on reclaimed land in central Taiwan." *Sino-Geotechnics 2000*, 77, 39−50 (in Chinese).

Zhang, G., Robertson, P. K., and Brachman, R. W. I. (2002). "Estimating liquefaction-induced ground settlements from CPT for level ground." *Canadian Geotechnical Journal*, 39, 1168−1180.

APPENDIX I

Formulae for Parameters I_c, q_{c1N}, r_d, MSF, and K_σ

The soil behavior type index I_c (dimensionless) is defined below, which is a variant of the definition provided by Lunne *et al.* (1997) and Robertson and Wride (1998):

$$I_c = [(3.47 - \log_{10} q_{c1N})^2 + (\log_{10} F + 1.22)^2]^{0.5} \quad (11)$$

where

$$F = f_s / (q_c - \sigma_v) \times 100\% \quad (12)$$

and where f_s is the sleeve friction (kPa), q_c is the cone tip resistance (kPa), σ_v is the total stress of the soil at the depth of concern (kPa), and q_{c1N} is the normalized tip resistance (dimen-

sionless). The term q_{c1N} is obtained through an iterative procedure involving the following equations (Idriss and Boulanger 2004):

$$q_{c1N} = C_N \, q_c / P_a \tag{13}$$

$$C_N = \left[\frac{P_a}{\sigma'_v} \right]^{\alpha} \leq 1.7 \tag{14}$$

$$\alpha = 1.338 - 0.249 \, (q_{c1N})^{0.264} \tag{15}$$

where P_a is the atmosphere pressure (kPa) and σ'_v is the effective stress of the soil at the depth of concern (kPa). The I_c values calculated with Eq. (11) generally agree well with those obtained from Robertson and Wride (1998) and Zhang *et al.* (2002); the difference between the two procedures is generally less than 5%.

The term r_d is the depth-dependent shear stress reduction factor (dimensionless) and is defined with the following equations (Idriss and Boulanger, 2004):

$$\ln(r_d) = \alpha + \beta M_w \tag{16}$$

$$\alpha = -1.012 - 1.126 \sin(5.133 + z/11.73) \tag{17}$$

$$\beta = 0.106 + 0.118 \sin(5.142 + z/11.28) \tag{18}$$

where z is the depth (m) and M_w is the moment magnitude (dimensionless).

The term MSF is the magnitude scaling factor (dimensionless) and is defined as (Idriss and Boulanger, 2004):

$$\text{MSF} = -0.058 + 6.9 \exp(-M_w / 4) \leq 1.8 \tag{19}$$

The term K_σ is the overburden correction factor (dimensionless) for CSR and is defined by the following equations (Idriss and Boulanger, 2004):

$$K_\sigma = 1 - C_\sigma \ln(\sigma'_v / P_a) \leq 1.0 \tag{20}$$

where

$$C_\sigma = \frac{1}{37.3 - 8.27 \, (q_{c1N})^{0.264}} \leq 0.3 \tag{21}$$